




Cite this: *Environ. Sci.: Adv.*, 2024, 3, 1309

## Enhancing ammonia recovery through pH polarization in bipolar membrane electro dialysis†

Sandali Panagoda,<sup>a</sup> Pengyi Yuan,<sup>b</sup> Vladimir Pavlovic,<sup>b</sup> John Barber<sup>b</sup> and Younggy Kim \*<sup>a</sup>

Ammonia recovery from food waste (including its liquid digestate) is highly emphasized in wastewater treatment and management. Among various membrane-based separation technologies, bipolar membrane electro dialysis (BMED) without anion exchange membranes (AEMs) is an attractive candidate for selective ammonia separation with reduced scaling problems. In this study, a bench-scale BMED stack was built using 5 pairs of cation exchange membranes (CEMs) and bipolar membranes (BPMs). A simulated food liquid digestate was treated using a lab-scale BMED stack to examine the ammonia separation with 3 different intermembrane distances (0.82, 1.64, and 2.46 mm). The highest electric current and ammonia separation were obtained for the intermembrane distance of 1.64 mm, while the BMED stack with 3 spacer gaskets (2.46 mm) still showed comparable separation performance without significant decreases in electric current or ammonia recovery. The residual  $\text{Ca}^{2+}$  and  $\text{Mg}^{2+}$  in the cleaning-in-place (CIP) solutions indicated that there were no noticeable scaling problems during the BMED operation. Finally, the pH polarization between the base and feed cells was found to minimize the ammonia back-diffusion even with the highly accumulated ammonia concentration ( $>11\,000\text{ mg}_\text{N}\text{ L}^{-1}$ ) in the base cell. With the relatively low energy requirement (1.24–6.78 kW h  $\text{kg}_\text{N}^{-1}$ ), BMED lacking AEMs with wide intermembrane distances was confirmed to be a sustainable candidate for ammonia recovery from wastewater with high levels of ammonia.

Received 14th March 2024  
Accepted 19th July 2024

DOI: 10.1039/d4va00082j

rsc.li/esadvances

### Environmental significance

Contamination of aquatic bodies with nitrogenous compounds causes eutrophication, which degrades the quality of water making it unfit for consumption and survival of aquatic life. Therefore, minimizing the entry of nitrogenous waste into natural waters is crucial in maintaining a healthy ecosystem. This research work focused on extracting ammonium in food liquid digestate prior to discharging to the environment. An ion exchange membrane-based separation technology called bipolar membrane electro dialysis was used to extract ammonium nitrogen. The results showed that this technology can accumulate ammonia up to  $11\,000\text{ mg}_\text{N}\text{ L}^{-1}$  without diffusive losses due to the pH polarization between the base and feed cells, proving it to be a sustainable candidate for ammonia separation from food liquid digestate.

## 1. Introduction

Anthropogenic discharge of nitrogenous compounds leads to adverse environmental effects including eutrophication, which has become one of the pressing environmental concerns worldwide. Algal blooms formed due to eutrophication prevent penetration of oxygen and sunlight, which ultimately results in deterioration of water quality and aquatic life. Therefore, prevention of eutrophication is important in maintaining a healthy aquatic ecosystem.<sup>1</sup> This can be achieved by reducing the entry of nitrogenous waste into the environment. Moreover,

the demand for nitrogen across the globe and stringent regulations on nitrogenous waste discharge to the environment can be met if nitrogenous compounds can be recovered from high-strength wastewater such as liquid digestate from the food industry. Food waste liquid digestate contains a significant concentration of ammonia ( $>5000\text{ mg}_\text{N}\text{ L}^{-1}$ ). The Haber–Bosch process is currently employed for ammonia production, which is energy-extensive and requires a significant carbon footprint as well.<sup>1,2</sup> Therefore, this study focused on efficient selective ammonia recovery as ammonium hydroxide from simulated food liquid digestate.

Bipolar membrane electro dialysis (BMED) can be used for acid and base production.<sup>3,4</sup> Moreover, BMED technology has been examined recently for the wastewater treatment industry<sup>5,6</sup> and recovery of ammonia using synthetic wastewater.<sup>7</sup> The production of protons in the BMED system prevents the scale formation in the feed reservoir and the hydroxide production

<sup>a</sup>Department of Civil Engineering, McMaster University, 1280 Main Street West, L8S 4L8, Hamilton, ON, Canada. E-mail: younggy@mcmaster.ca

<sup>b</sup>Veolia Water Technologies & Solutions, Guelph, Ontario, Canada

† Electronic supplementary information (ESI) available. See DOI: <https://doi.org/10.1039/d4va00082j>



accelerates scaling in the base reservoir. Therefore, anion exchange membranes (AEMs), which are more susceptible to fouling were replaced by bipolar membranes (BPMs) to avoid scaling and fouling problems in conventional electrodialysis (ED) systems, and also separation of anions was of no interest in this study.

A single cell pair of the BMED stack employed in this study consists of a feed cell and a base cell separated by a cation exchange membrane (CEM) and a BPM. Spacers are placed between the ion exchange membranes (IEMs) and BPMs to provide space for the solutions to flow inside the cell by maintaining the intermembrane distance. Mixing of solutions in the cells is also facilitated by the presence of spacers, intensifying mass transfer by thinning the boundary layer.<sup>8,9</sup> The spacer thickness also affects the stack resistance. The resistance of the BMED stack increases with increasing spacer thickness.<sup>8</sup> The high conductivity of high strength wastewater (feed compartment) and production of hydroxides in the base compartment during BMED operation assist in overcoming the resistance created by the spacers unlike conventional ED. Therefore, the intermembrane distance can be larger for BMED operation in comparison to conventional ED. Furthermore, when the spacer thickness is too small, a restriction for the flow of digested sludge in the narrow cells can limit practical ED and BMED applications for nutrient recovery. Moreover, Zhong *et al.*<sup>9</sup> suggested the use of two spacers to increase the intermembrane distance for practical ED applications. However, thinner spacers in the base cell are preferable in this study as the conductivity of the base solution was relatively low in comparison to the feed solution. Therefore, the ohmic resistance in the base cells needs to be minimized with the use of the thinner spacer (0.82 mm). Moreover, the effect of intermembrane distance in BMED systems on ammonia recovery has not yet been studied. Thus, this study also attempts to investigate the optimal intermembrane distance of the BMED stack for efficient ammonia recovery.

Another important objective of this work is to investigate the role of pH polarization in ammonia separation. In BMED lacking AEMs, the base cell pH increases above the  $pK_a$  of ammonium ions (9.4). As a result, ammonium ions transferred from the feed cell are converted into electrically neutral ammonia. We hypothesize that this pH polarization across the CEM can be used to slow down the potential back diffusion of ammonia from the base to the feed.

## 2. Materials and methods

### 2.1 Setting up the BMED

A bench-scale BMED stack (Fig. 1) was constructed using 5 CEMs (CR62T, Veolia Water Technologies & Solutions, Canada) and 5 BPMs (AR103N and CR61, Veolia Water Technologies & Solutions, Canada).<sup>2,10</sup> An extra AEM (AR103N, Veolia Water Technologies & Solutions, Canada) and a CEM (CR62T, Veolia Water Technologies & Solutions, Canada) were placed near the anode and cathode chambers, respectively, to prevent the transfer of ions in the feed reservoir to the electrode rinse reservoir. The BMED stack consisted of feed and base channels

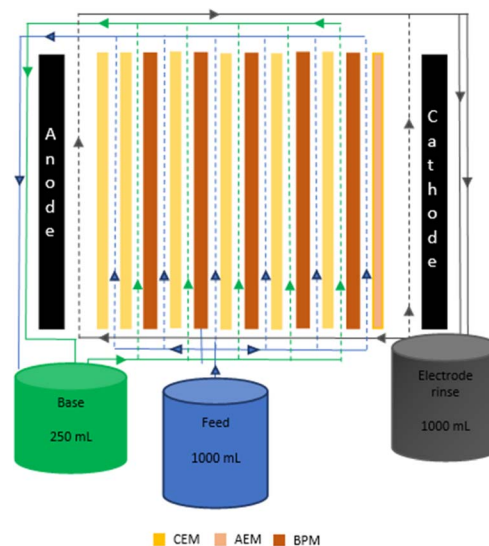


Fig. 1 BMED stack configuration and flow inside the stack.

Table 1 Physicochemical properties of IEMs supplied by the manufacturer

Property	CR62T	AR103N	BPM
Thickness (mm)	0.32	0.38–0.42	1.1
Burst strength (psi)	85	95	
Ion-exchange capacity (meq per gram of dry membrane)	2.60	2.37	
Resistivity in 0.5 N NaCl at 25 °C ( $\Omega \text{ cm}^2$ )	6	3.48	
Permselectivity (%)	97	92	
pH operation range	1–14	1–14	1–14
Maximum current density ( $\text{mA cm}^{-2}$ )	32.5	32.5	32.5

(Fig. 1) as acid stream was not present due to lack of AEMs. The intermembrane distance in the stack was maintained using polyethylene mesh spacers of the overall dimensions  $16.5 \times 7.5 \text{ cm}^2$  with an effective IEM surface area of  $36.7 \text{ cm}^2$  ( $10.5 \times 3.5 \text{ cm}^2$ ). Titanium plates coated with platinum were used as electrodes. The physicochemical properties of IEMs are shown in Table 1.

### 2.2 BMED operation

The system was operated using an electric field provided by the anode and the cathode which were connected to an external power supplier (Model 9201, BK Precision, USA). A synthetic feed solution representative of liquid digestate from food waste was prepared in the lab. The composition used for preparation is given in Table 2. Note that we assumed the liquid digestate of food waste for the feed solution. The BMED operation was carried out with 1000 mL of synthetic feed solution and 250 mL of deionized water as the base reservoir to recover ammonium hydroxide with maximum purity. A volume of 1000 mL of 0.1 M  $\text{Na}_2\text{SO}_4$  was used as the electrode rinse solution. The system was operated for 90 minutes allowing recirculation of all three solutions using peristaltic pumps which were connected



Table 2 Composition of the synthetic food liquid digestate

Parameter	Average and standard deviation	Ref.
Ammonium chloride	5000.00 ± 0.001 mg L <sup>-1</sup>	11
Calcium chloride	88.78 ± 0.001 mg L <sup>-1</sup>	12
Magnesium chloride	95.21 ± 0.001 mg L <sup>-1</sup>	13
Sodium bicarbonate	8400.00 ± 0.001 mg L <sup>-1</sup>	14
Sodium chloride	409.08 ± 0.001 mg L <sup>-1</sup>	15
Potassium chloride	149.10 ± 0.001 mg L <sup>-1</sup>	14
pH	7.86 ± 0.049	—
Conductivity	49.11 ± 0.276 mS cm <sup>-1</sup>	—

separately to each reservoir. Deionized water was circulated in the stack prior to starting the experiments for five minutes to eliminate the air bubbles trapped inside. The linear velocity of the feed and base channels was maintained at 1.61 cm s<sup>-1</sup> and the electrode rinse at 4.65 cm s<sup>-1</sup> throughout the operation. Duplicate experiments were performed at five different voltages by varying the intermembrane distance in the feed compartment. The intermembrane distance of the feed cell was manipulated by using 1, 2, or 3 gasket(s) and spacer(s) between IEMs. When a single gasket/spacer was placed in the feed cell, the chamber thickness was 0.82 mm. Introducing two gaskets/spacers resulted in a cell thickness of 1.64 mm, while three gaskets/spacers increased the cell thickness to 2.46 mm. Throughout all experiments, the thickness of the base cell remained constant at 0.82 mm. The linear water flow velocity of the feed cell was maintained constant by increasing the flow rate according to the intermembrane distances.

### 2.3 Clean-in-place (CIP)

The clean-in-place procedure (CIP) was carried out by using 5% HCl followed by 5% NaCl for 30 minutes by alternating the flow direction every 15 minutes. The BMED stack was cleaned using 6 L of deionized water before and after the CIP. The cations in the CIP solutions from the feed and base after completion of experiments with 2.46 mm intermembrane distance were quantified to investigate the scaling in the chambers.

### 2.4 Voltage drop per cell pair

The voltage drop at the electrodes was found by assembling a stack with the electrodes, 1 CEM (CR62T, Veolia Water Technologies & Solutions, Canada), and 1 AEM (AR103N, Veolia Water Technologies & Solutions, Canada). The reservoirs used were feed (1000 mL of synthetic solution) and electrode rinse (1000 mL of 0.1 M Na<sub>2</sub>SO<sub>4</sub>) only. The voltage applied was increased every three minutes, and the average current was found (Fig. S4†). The cell pair voltage was determined using the following equation.

$$\text{Cell pair voltage drop (V)} = \frac{E^{\text{total}} - E^{\text{electrodes}}}{\text{Number of cell pairs}}$$

where  $E^{\text{total}}$  is the total voltage applied to the stack, while  $E^{\text{electrodes}}$  is the voltage consumed by the electrodes.

Table 3 Composition of the reactors used in back diffusion experiments

	Low ammonia cell (initial pH)	High ammonia cell (initial pH)
Test 1	NaHCO <sub>3</sub> (6.4)	0.357 M NH <sub>4</sub> OH (11.2)
Test 2	0.4 M NaOH (13.6)	0.357 M NH <sub>4</sub> OH (11.2)
Test 3	0.4 M NaHCO <sub>3</sub> (6.5)	0.357 M NH <sub>4</sub> Cl (6.3)

### 2.5 Back-diffusion experiments

Three bench-scale reactors were built using polypropylene blocks. In the reactor, two cells (each 15 mL) were separated by a CEM (CR62T, Veolia Water Technologies & Solutions, Canada), where one cell was a low ammonia cell and the other one was a high ammonia cell (Table 3). In this experiment, the effect of pH in these cells on the back-diffusion of ammonia from the high to low ammonia cell depending on whether ammonia is present as NH<sub>4</sub><sup>+</sup> or NH<sub>3</sub> was examined.

### 2.6 Experimental analysis

Experimental measurements such as pH, conductivity (Orion Versa Star, Thermo Scientific, USA) and ammonia concentration (Ammonia test kits, Method 10 205, Hach Company, USA) were obtained at 0, 30, 60, and 90 minutes in the feed and base samples collected from voltage application experiments. The samples (including CIP) were further analysed using Inductively Coupled Plasma-Optical Emission Spectroscopy (ICP-OES, Vista Pro, Varian Inc., Australia) for other cations, namely, Ca<sup>2+</sup>, Mg<sup>2+</sup>, and K<sup>+</sup>. Prior to ICP-OES analysis, the samples were treated with 70% nitric acid (w/w) and then filtered using syringe filters with a pore size of 0.45 μm (polyethersulfone membrane, VWR International, USA). Samples from the low ammonia side in each reactor from the back-diffusion experiments were collected every 30 minutes, and ammonia concentration (Ammonia test kits, Method 10 205, Hach Company, USA), pH (Orion Versa Star, Thermo Scientific, USA) and conductivity (Orion Versa Star, Thermo Scientific, USA) of the samples were measured.

### 2.7 Energy requirement

The energy requirement (kW h kg<sub>N</sub><sup>-1</sup>) of the BMED stack was calculated using the following equation. The energy pertaining to pumping is not considered as it is relatively low in comparison to the energy used for voltage applications in BMED.<sup>16</sup>

$$\text{Energy consumption} = \frac{\sum E^{\text{applied}} I_t \Delta t}{3600 \times (C_{F_0} V_{F_0} - C_{F_t} V_{F_t})}$$

where  $E^{\text{applied}}$  (V) is the voltage applied for a single experiment,  $I_t$  (A) is the electric current at time  $t$ , and  $\Delta t$  (s) is the time interval.  $C_{F_0}$  (kg L<sup>-1</sup>) and  $C_{F_t}$  (kg L<sup>-1</sup>) are the free ammonia concentration in the feed solution at time 0 and  $t$ .  $V_{F_0}$  (L) and  $V_{F_t}$  (L) are the volumes of the feed reservoir at times 0 and  $t$ .



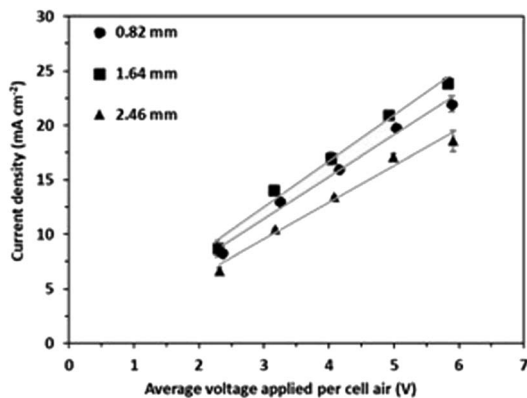


Fig. 2 Change in average current density with average voltage applied with 0.82, 1.64, and 2.46 mm intermembrane distances.

### 3. Results and discussion

#### 3.1 Effect of intermembrane distance on current density

The highest current density was observed consistently for an intermembrane distance of 1.64 mm (*i.e.*, two gaskets between IEMs) (Fig. 2). For instance, the average current density with 2 gaskets was higher by 8.2% compared to that with a single gasket between IEMs and higher by 22.4% compared to that with three gaskets in the feed cell for the voltage application of 6 V per cell pair. It should be emphasized that the feed flow velocity was consistent at  $1.61 \text{ cm s}^{-1}$  for the 3 different intermembrane distance conditions; thus, the hydrodynamic mixing condition can hardly explain this result. However, the relatively fast water flow velocity ( $1.61 \text{ cm s}^{-1}$ ) facilitated sufficient mass transfer in the BMED cells. Furthermore, the feed solution consistently showed very high conductivity due to acid production at the bipolar membrane. The feed solution conductivity decreased slightly from  $49.30$  to  $43.80 \text{ mS cm}^{-1}$  over the 90 minute experiments at 6 V per cell pair (Fig. S3†), resulting in a negligible electric potential drop in the bulk phase. For instance, the current density of  $20 \text{ mA cm}^{-2}$  required voltage consumptions of 0.1569, 0.1620 and  $0.1545 \text{ V}$  in the 0.82, 1.64, and 2.46 mm thick feed cells, respectively, according to Ohm's law. Considering the cell pair voltage of 5.83–5.91 V, these voltage consumptions in the feed cell are practically

negligible (only 2.61–2.79% of the applied voltage per cell pair). Thus, the high conductivity of the feed solution resulted in negligible differences in the electric current density.<sup>17</sup> This observation was valid for the large intermembrane distance of up to 2.46 mm.

The concentration of ammonia in food waste typically ranges from  $7000$  to  $20\,000 \text{ mg}_N \text{ L}^{-1}$ , and the resulting leachate has been observed to contain ammonia within the range of  $1000$  to  $2000 \text{ mg}_N \text{ L}^{-1}$ .<sup>18</sup> This high ammonia concentration along with high conductivity allowed the use of thicker feed cells up to 2.46 mm in this study. Furthermore, food waste digestate inevitably contains high solid concentrations. As only charged ions are transferred towards the electrodes through the membranes, BMED applications do not require intensive pretreatment in comparison to other treatment technologies such as RO and NF.<sup>19</sup>

In addition, digested food waste sludge can even be directly introduced into BMED stacks for ammonia separation if the cell thickness is 2.5 mm or thicker as also previously reported.<sup>20</sup> Therefore, the use of BMED with a thick inter-IEM distance can be broadly applied for effective ammonia separation from digested food waste.

#### 3.2 Effect of intermembrane distance on ammonia recovery

The highest ammonia removal of 81.3% was achieved at 35 V with two gaskets in the feed cells, while it was 79.8% with a single gasket and 72.2% with three gaskets (Fig. 3). This finding is consistent with the current density results as the maximum current density was obtained with two gaskets in the feed cell. It should be noted that the ammonia removal in the feed reservoir was used for the separation efficiency (not the ammonia accumulation in the base reservoir) due to the ammonia loss by volatilization from the base reservoir. The base pH was increased up to 10.9 (Fig. S2†), and the total ammonia concentration was above  $11 \text{ g}_N \text{ L}^{-1}$ , resulting in volatilization losses from the base reservoir as previously reported.<sup>10</sup> The ammonia removal rate was faster in the first 30 minutes, but it declined afterwards (Fig. 3). Also, the ammonia removal rate became almost constant regardless of the applied voltage in the last 30 minutes as the feed concentration profiles have similar slopes. This observation can be explained by the significant concentration gradient between the feed and the base.<sup>2</sup>

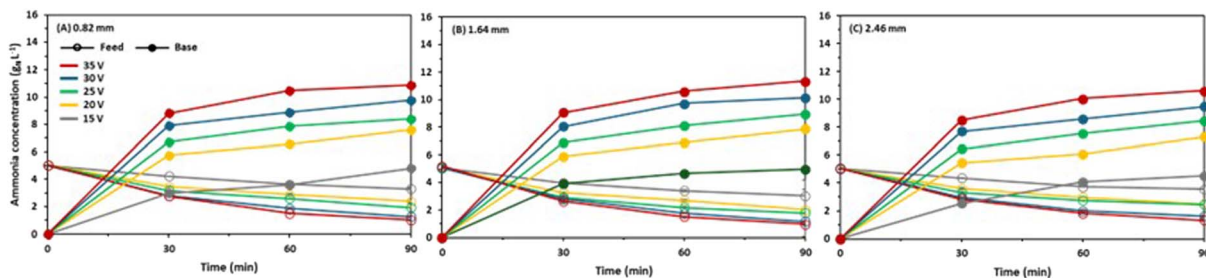


Fig. 3 Change in ammonia concentration of feed and base reservoirs over time at different voltage applications with (A) 0.82, (B) 1.64, and (C) 2.46 mm intermembrane distances.



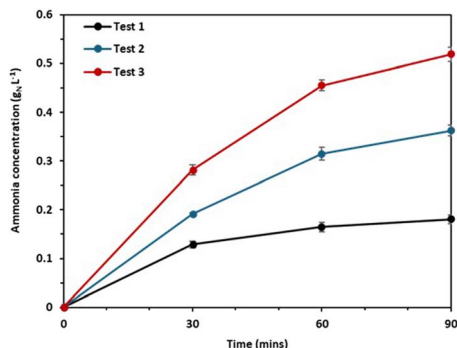


Fig. 4 Ammonia concentration in the low concentration cell of the back-diffusion test; test 1:  $\text{NaHCO}_3$  and  $\text{NH}_4\text{OH}$ ; test 2:  $\text{NaOH}$  and  $\text{NH}_4\text{OH}$ ; test 3:  $\text{NaHCO}_3$  and  $\text{NH}_4\text{Cl}$ .

Another factor affecting slow ammonia recovery during the last 30 minutes is the transfer of  $\text{H}^+$  through the CEM. However, considering the feed and base pH, the  $\text{H}^+$  leakage through the CEM must be negligible compared to ammonia back diffusion. Regarding electroosmosis, the feed volume was decreased from 1000 mL to 972 mL (35 V application with 1.64 mm intermembrane distance). This water transport is likely to be driven by electroosmosis as osmotic water transport was minor because of the relatively short operation (90 min). Back-diffusion of ammonia due to non-ideal nature of the CEM can explain the slowed separation of ammonia for the last 30 minutes of BMED operation.

### 3.3 pH Polarization between the feed and the base

It should be noted that the separation of ammonia continued (negative slopes of the feed concentration in Fig. 3) even though the base ammonia concentration reached  $11 \text{ g}_\text{N} \text{ L}^{-1}$ .

The pH polarization across CEMs led to alkaline pH in the base cell due to the creation of hydroxide ions in the BPM (Fig. S2<sup>†</sup>). This alkaline pH converts ammonium ions (transferred from the feed cell) into electrically neutral free ammonia. This ammonia speciation due to the pH polarization is responsible for successful prevention of ammonia back-diffusion even with a high ammonia concentration in the base cell.

A separate experiment was conducted, and we found that the pH polarization plays an important role in preventing ammonia back diffusion in the BMED separation (Fig. 4).

The reaction of  $\text{NH}_4^+$  with  $\text{OH}^-$  produces both  $\text{NH}_3$  and water ( $\text{H}_2\text{O}$ ). The additional water formed can contribute to an increase in the total volume of the solution, thereby inevitably diluting the concentrations of other solutes present. Furthermore, when  $\text{NH}_3$  is formed in the solution, it subsequently volatilizes reducing the total concentration of solutes, causing a dilution effect. To mitigate the loss of ammonia to the atmosphere by volatilization, a closed system design should be considered.

### 3.4 Cation competition on ammonia recovery

The individual cationic separation was similar between the intermembrane distances of 0.82 and 1.64 mm, while 1.64 mm showed the highest separation efficiency for all voltage applications (Fig. 5). This can be explained with comparatively high current densities for the intermembrane distance of 1.64 mm. The cation with the highest separation efficiency at 30 and 35 V was found to be  $\text{K}^+$  for all three intermembrane distances, followed by  $\text{NH}_4^+$ . However, for the lower voltage applications (15, 20, and 25 V), the separation efficiency of  $\text{NH}_4^+$  was higher than that of  $\text{K}^+$  for all intermembrane distances. This trend can be explained as the CEM in the BMED stack (CR62T) is more favourable for mono-valent separation.<sup>10</sup>

The ammonia separation was faster than  $\text{K}^+$  for the low voltage applications (15, 20, and 25 V). In contrast, in the high voltage applications (30 and 35 V), the separation of  $\text{NH}_4^+$  proceeded at a slower rate compared to the  $\text{K}^+$  separation despite the similar equivalent ionic conductivities of  $\text{K}^+$  and  $\text{NH}_4^+$  ( $0.00735 \text{ m}^2 \text{ S mol}^{-1}$ ).<sup>21</sup> Although additional experiments are necessary to clarify this observation, the CEM selectivity and concentration polarization in the feed-side boundary near the CEM are thought to affect this competitive separation between  $\text{K}^+$  and  $\text{NH}_4^+$ . For instance, for the low voltage applications, the CEM selectivity had a more dominant effect on the competition and *vice versa* for the high voltage applications.

### 3.5 Scaling in BMED

The residual concentrations of  $\text{Ca}^{2+}$  and  $\text{Mg}^{2+}$  in the CIP solutions were below 3%, indicating that the precipitation of salts of  $\text{Ca}^{2+}$  and  $\text{Mg}^{2+}$  during BMED operation was not significant. However, the residual concentrations of  $\text{Ca}^{2+}$  and  $\text{Mg}^{2+}$  in the CIP solution were found to be higher in the base reservoir than in the feed reservoir (Fig. 6). This can be explained by

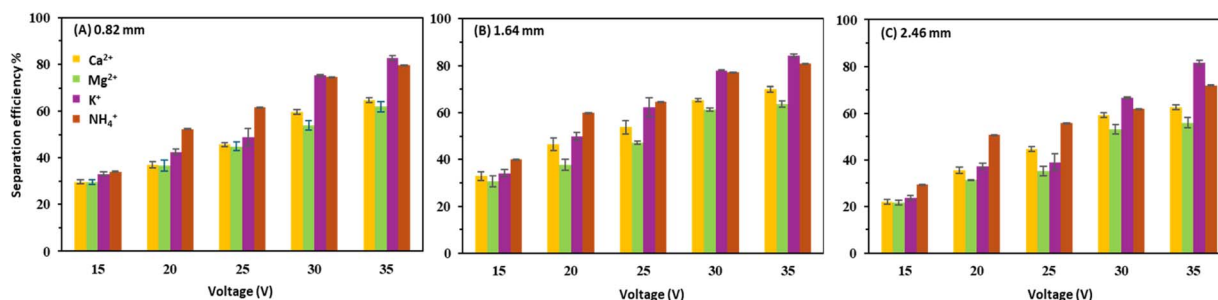


Fig. 5 Removal efficiency of cations at different voltage applications with (A) 0.82, (B) 1.64, and (C) 2.46 mm intermembrane distances.



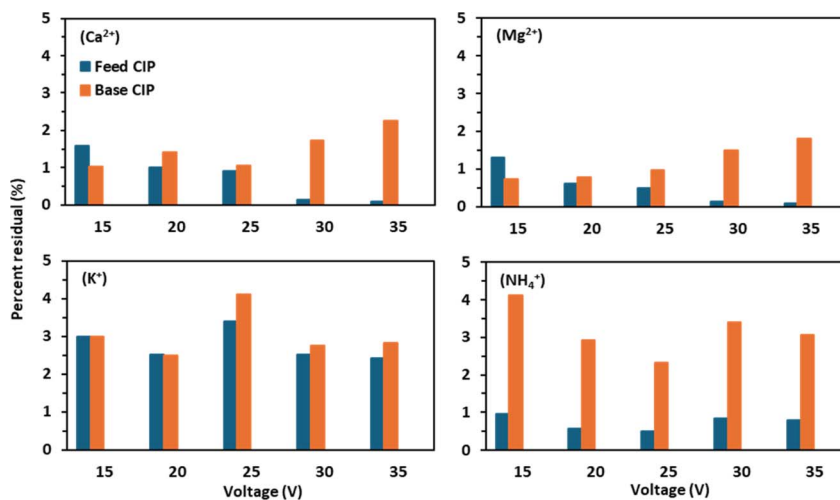


Fig. 6 Percent residual of cations in feed and base channels found in CIP solutions.

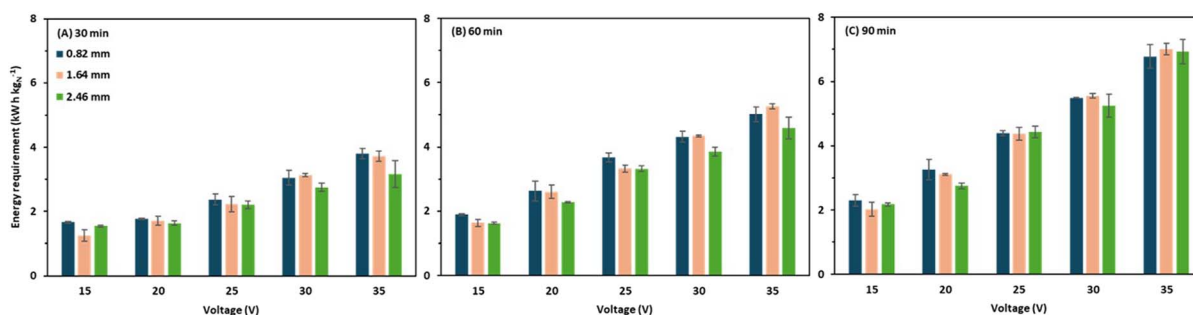


Fig. 7 Energy requirement of the membrane stack at (A) 30 minutes of operation, (B) 60 minutes of operation, and (C) 90 minutes of operation.

concentration polarization on the base side due to the formation of steep concentration gradients. Concentration polarization promotes deposition of Ca<sup>2+</sup> and Mg<sup>2+</sup> precipitates on the membrane surface at the base side.<sup>16</sup> The generation of OH<sup>-</sup> ions due to water splitting at the bipolar membrane junction was greatly induced at high voltage applications promoting deposition of hydroxides of Ca<sup>2+</sup> and Mg<sup>2+</sup>.<sup>2</sup> In a previous study conducted by Guo *et al.*,<sup>2</sup> with dewatering centrate, they observed greater amounts of precipitation ranging 48–59% of Ca<sup>2+</sup> and 36–43% of Mg<sup>2+</sup> in the CIP solutions in comparison to the initial mass of Ca<sup>2+</sup> and Mg<sup>2+</sup> in the dewatering centrate. The substantially low precipitation of Ca<sup>2+</sup> and Mg<sup>2+</sup> in this study can be explained by the high affinity of the CEM to NH<sub>4</sub><sup>+</sup> compared to Ca<sup>2+</sup> and Mg<sup>2+</sup>. This can be further demonstrated by the slight drop in conductivity of the feed reservoir (Fig. S3†) at the end of experiments implying rapid NH<sub>4</sub><sup>+</sup> transfer through the CEMs compared to di-valent cations.<sup>10</sup> The residual concentrations of K<sup>+</sup> and NH<sub>4</sub><sup>+</sup> in the CIP solutions were found to be below 5%, and the precipitation of K<sup>+</sup> and NH<sub>4</sub><sup>+</sup> salts was not a concern in our study as they are highly soluble.

### 3.6 Energy requirement

The total energy requirement ranged widely from 0.8 to 5.3 kWh kg<sup>-1</sup> depending on the applied voltage, operation time, and

intermembrane distance (Fig. 7). In a previous study, the average energy requirement for BMED operation in ammonia recovery varied between 7 and 16 kWh kg<sup>-1</sup> with an ammonia recovery of 95%.<sup>10</sup> In another study, an energy requirement of 9.6–24.2 kWh kg<sup>-1</sup> was reported for an ammonia recovery of 70%.<sup>2</sup> A recent study conducted by Guo *et al.*<sup>22</sup> obtained an ammonia recovery of 74% with an energy requirement of 8.12–11.9 kWh kg<sup>-1</sup>. Furthermore, a low energy requirement of 4.5 kWh kg<sup>-1</sup> was achieved by Ali *et al.*,<sup>23</sup> by employing a bench-scale BMED stack; however, the ammonia recovery was only 50% over an operation period of 120 minutes. Therefore, the energy requirement for the thick intermembrane distance (up to 2.46 mm) was still comparable to those reported in previous BMED studies.

### 3.7 Fouling control in BMED

Fouling was not a significant concern in this study due to the absence of soluble COD or large particulate materials in the feed solution. However, the use of AEMs was minimized in this study (except at the cathode terminal) as there was no interest in anion separation and to avoid fouling problems. The stable current densities obtained in the separation experiments showed that both scaling and fouling problems did not influence the overall performance of the BMED stack (Fig. S1†).



## 4. Conclusions

BMED constituting CEMs and BPMs was investigated for efficient ammonia recovery from simulated food liquid digestate. Different voltages were applied to recover ammonia by increasing the intermembrane distance from 0.82, 1.64, and 2.46 mm to identify the optimal intermembrane distance for efficient recovery of ammonia. The results showed that 0.82 and 1.64 mm intermembrane distances work best for ammonia recovery, while the 1.64 mm intermembrane distance showed the highest recovery efficiency. However, the reduction in ammonia recovery efficiency was not very significant with the 2.46 mm intermembrane distance. Therefore, we concluded that the intermembrane distance can be increased up to 2.46 mm in BMED operations for treating food liquid digestate. Another key finding of this study was that the pH polarization across the CEMs assists in minimizing the back-diffusion of ammonia. The alkaline pH in the base reservoir helped the formation of electrically neutral ammonia which was incapable of diffusing back through the CEMs. Furthermore, the neutral pH in the feed reservoir reduced the back-diffusion of ammonia in contrast to alkaline pH. In cation separation tests, the 1.64 mm intermembrane distance displayed the highest cation separation efficiency.  $K^+$  was separated rapidly at higher voltage applications than  $NH_4^+$ , while at lower voltage applications,  $NH_4^+$  separation was dominant over  $K^+$ . The results of scaling tests indicated very low residual concentrations (<3%) of salt forming cations such as  $Ca^{2+}$  and  $Mg^{2+}$ , which confirmed that the regular CIP procedure was successful in reducing scale formation. The energy requirement of the BMED stack with the wider intermembrane distances (up to 2.46 mm) was found to be analogous to previous studies, which were significantly low in comparison to traditional ammonia production processes such as Haber–Bosch. Therefore, efficient separation of  $NH_4^+$  from high strength wastewater can be achieved using BMED technology, thereby reducing the nitrogen load in the environment while meeting the nitrogen demand of various industries.

## Conflicts of interest

The authors declare no conflict of interest.

## Acknowledgements

This study was funded by the Natural Sciences and Engineering Research Council of Canada (Discovery Grants, RGPIN-2019-06747 & Discovery Accelerator Supplement, RGPAS-2019-00102) and Ontario Ministry of Research and Innovation (Ontario Research Fund-Research Excellence, RE09-077). The authors thank Ms Monica Han for her support in analytical equipment operation.

## References

- 1 Y. Li, R. Wang, S. Shi, H. Cao, N. Y. Yip and S. Lin, Bipolar Membrane Electrodialysis for Ammonia Recovery from Synthetic Urine: Experiments, Modeling, and Performance Analysis, *Environ. Sci. Technol.*, 2021, **55**(21), 14886–14896.
- 2 H. Guo, P. Yuan, V. Pavlovic, J. Barber and Y. Kim, Ammonium sulfate production from wastewater and low-grade sulfuric acid using bipolar- and cation-exchange membranes, *J. Cleaner Prod.*, 2021, **285**, 124888, DOI: [10.1016/j.jclepro.2020.124888](https://doi.org/10.1016/j.jclepro.2020.124888).
- 3 M. Bailly, Production of organic acids by bipolar electrodialysis: Realizations and perspectives, *Desalination*, 2002, **144**(1–3), 157–162.
- 4 K. Song, S. C. Chae and J. H. Bang, Separation of sodium hydroxide from post-carbonation brines by bipolar membrane electrodialysis (BMED), *Chem. Eng. J.*, 2021, **423**, 130179.
- 5 F. Gao, L. Wang, J. Wang, H. Zhang and S. Lin, Nutrient recovery from treated wastewater by a hybrid electrochemical sequence integrating bipolar membrane electrodialysis and membrane capacitive deionization, *Environ. Sci.: Water Res. Technol.*, 2020, **6**(2), 383–391.
- 6 W. Tian, X. Wang, C. Fan and Z. Cui, Optimal treatment of hypersaline industrial wastewater via bipolar membrane electrodialysis, *ACS Sustain. Chem. Eng.*, 2019, **7**(14), 12358–12368.
- 7 Y. Li, S. Shi, H. Cao, X. Wu, Z. Zhao and L. Wang, Bipolar membrane electrodialysis for generation of hydrochloric acid and ammonia from simulated ammonium chloride wastewater, *Water Res.*, 2016, **89**, 201–209.
- 8 Y. Kim, W. S. Walker and D. F. Lawler, Electrodialysis with spacers: Effects of variation and correlation of boundary layer thickness, *Desalination*, 2011, **274**(1–3), 54–63, DOI: [10.1016/j.desal.2011.01.076](https://doi.org/10.1016/j.desal.2011.01.076).
- 9 X. W. Zhong, W. R. Zhang, Z. Y. Hu and H. C. Li, Effect of characterizations of spacer in electrodialysis cells on mass transfer, *Desalination*, 1983, **46**(1–3), 243–252.
- 10 M. Mohammadi, H. Guo, P. Yuan, V. Pavlovic, J. Barber and Y. Kim, Ammonia separation from wastewater using bipolar membrane electrodialysis, *Electrochem. Sci. Adv.*, 2021, **1**(4), 1–8.
- 11 L. Maya-Altamira, A. Baun, I. Angelidaki and J. E. Schmidt, Influence of wastewater characteristics on methane potential in food-processing industry wastewaters, *Water Res.*, 2008, **42**(8–9), 2195–2203.
- 12 G. G. Kurup, B. Adhikari and B. Zisu, Treatment performance and recovery of organic components from high pH dairy wastewater using low-cost inorganic ferric chloride precipitant, *J. Water Process Eng.*, 2019, **32**, 100908, DOI: [10.1016/j.jwpe.2019.100908](https://doi.org/10.1016/j.jwpe.2019.100908).
- 13 A. Eftaxias, V. Diamantis and A. Aivasidis, Anaerobic digestion of thermal pre-treated emulsified slaughterhouse wastes (TESW): Effect of trace element limitation on process efficiency and sludge metabolic properties, *Waste Manag.*, 2018, **76**, 357–363, DOI: [10.1016/j.wasman.2018.02.032](https://doi.org/10.1016/j.wasman.2018.02.032).
- 14 J. A. McGarvey, W. G. Miller, S. Sanchez, C. J. Silva and L. C. Whitehand, Comparison of bacterial populations and chemical composition of dairy wastewater held in circulated and stagnant lagoons, *J. Appl. Microbiol.*, 2005, **99**(4), 867–877.



- 15 (a) M. El-Fadel, E. Bou-Zeid, W. Chahine and B. Alayli, Temporal variation of leachate quality from pre-sorted and baled municipal solid waste with high organic and moisture content, *Waste Manag.*, 2002, **22**, 269–282; (b) M. Neugebauer and P. Sołowiej, The use of green waste to overcome the difficulty in small-scale composting of organic household waste, *J. Cleaner Prod.*, 2017, **156**, 865–875.
- 16 H. Strathman, *Ion Exchange Membrane Processes*.
- 17 Y. Liu, X. Wu, X. Wu, L. Dai, J. Ding, X. Ye, *et al.*, Recovery of nickel, phosphorus and nitrogen from electroless nickel-plating wastewater using bipolar membrane electrodialysis, *J. Cleaner Prod.*, 2023, **382**, 135326, DOI: [10.1016/j.jclepro.2022.135326](https://doi.org/10.1016/j.jclepro.2022.135326).
- 18 S. Y. Xu, O. P. Karthikeyan, A. Selvam and J. W. C. Wong, Microbial community distribution and extracellular enzyme activities in leach bed reactor treating food waste: Effect of different leachate recirculation practices, *Bioresour. Technol.*, 2014, **168**, 41–48, DOI: [10.1016/j.biortech.2014.05.009](https://doi.org/10.1016/j.biortech.2014.05.009).
- 19 Y. Tanaka, Chapter 7 Donnan Dialysis, in *Membrane Science and Technology*, 2007, pp. 495–503.
- 20 B. Ebbers, L. M. Ottosen and P. E. Jensen, Electrodialytic treatment of municipal wastewater and sludge for the removal of heavy metals and recovery of phosphorus, *Electrochim. Acta*, 2015, **181**, 90–99, DOI: [10.1016/j.electacta.2015.04.097](https://doi.org/10.1016/j.electacta.2015.04.097).
- 21 L. E. Richter, A. Carlos, and D. M. Beber, *CRC Handbook of Chemistry and Physics*, CRC Press, New York, 97th edn, 2017.
- 22 X. Guo, J. Chen, X. Wang, Y. Li, Y. Liu and B. Jiang, Sustainable ammonia recovery from low strength wastewater by the integrated ion exchange and bipolar membrane electrodialysis with membrane contactor system, *Sep. Purif. Technol.*, 2023, **305**, 122429, DOI: [10.1016/j.seppur.2022.122429](https://doi.org/10.1016/j.seppur.2022.122429).
- 23 M. A. B. Ali, M. Rakib, S. Laborie, P. Viers and G. Durand, Coupling of bipolar membrane electrodialysis and ammonia stripping for direct treatment of wastewaters containing ammonium nitrate, *J. Membr. Sci.*, 2004, **244**(1–2), 89–96.

